Computational Study of Secondary Hole Effect on Film Cooling

Leandro Marochio Fernandes, leandro.mf@ig.com.br
Rômulo Bessi Freitas, romulodnj@hotmail.com
Márcio Teixeira de Mendonça, marcio@ita.br
Instituto Tecnológico de Aeronáutica, Pç. Mal. Eduardo Gomes, 50. 12228-900, São José dos Campos, Brazil
Ricardo B. Flatschart, ricardo.flatschart@vse.com.br
Aloísio V. Pantaleão, aluisio.pantaleao@vse.com.br
Vale Soluções em Energia, Rod. Presidente Dutra, km 138. 12247-004, São José dos Campos, Brazil

Abstract. *In gas turbines higher specific power and lower specific fuel consumption can be achieved increasing the turbine entry temperature (TET). Higher TET may result in significant savings in fuel which translates into thousands of Dollars per year. That justifies the investments in the development of new high temperature resistant alloys and improved cooling systems. through the years the TET has increased from around 1200 K in the early 60s to as high as 1850 K nowadays. The first cooling methods were based on convective cooling, but the limitations associated with relative low values of convective cooling coefficients and high blade surface temperature result in TET limitation of around 1600 K. A much more efficient technique would result if the blade surface is isolated from the hot gases by a cooling film, which is ejected over the blade through film cooling holes. Film cooling is a complex technique that depends on the interaction between the main hot stream and the cooling jet. A cooling effectiveness parameter is used as the measure of how much the cooling flow is mixed with the main stream and varies from 1 close to the cooling hole and 0 downstream. The effectiveness depends on a large number of parameters, most of theme associated with the flow topology of a jet into a cross flow. A jet issuing from a wall into a main stream is bent in the direction of the flow and develop into a pair of counter rotating vortices that pump low temperature fluid away from the wall and high temperature fluid close to the wall. Most of the research in cooling configurations are associated with ways to reduce the development of these counter rotating vortices such as trenches, shaped holes, compound angle holes and secondary anti-vortex holes. The present investigation build on previous research on film cooling effectiveness. A system consisting of two holes place in line with the main stream is investigated in order to access the effect of their interaction on the temperature distribution downstream. The development of counter rotating vortices in the upstream hole will change the flow field due to the downstream hole, which may have an adverse effect on the film cooling effectiveness. Rows of holes are used to provide enhanced cooling in localized regions and the present investigation addresses the question of which will be the resulting flow field and cooling capability when such configuration is employed. The test configuration considers a smaller hole upstream and different mass flow ration distribution between the two holes. The results show that the upstream flow deflects the main stream resulting in the development of the characteristic counter rotating vortices. Theses vortices lift up the downstream cooling flow of the second hole and reduce the cooling effectiveness. A open source control volume based solver (Open∇Foam) is used to solve the compressible Reynolds Average Navier-Stokes equations and a turbulent model is used to close the system of equations.*

Keywords: *gas turbine cooling, film cooling, Numerical simulation, gas turbine*

1. INTRODUCTION

In gas turbines higher specific power and lower specific fuel consumption can be achieved increasing the turbine entry temperature (TET). Higher TET may result in significant savings in fuel which translates into thousands of Dollars per year. That justifies the investments in the development of new high temperature resistant alloys and improved cooling systems. Through the years the TET has increased from around 1200 K in the early 60s to as high as 1850 K nowadays. The first cooling methods were based on convective cooling, but the limitations associated with relative low values of convective cooling coefficients and high blade surface temperature result in TET limitation of around 1600 K. A much more efficient technique would result if the blade surface is isolated from the hot gases by a cooling film, which is ejected over the blade through film cooling holes.

Film cooling is a complex technique that depends on the interaction between the main hot stream and the cooling jet. A cooling effectiveness parameter η is used as the measure of how much the cooling flow is mixed with the main stream and varies from $\eta = 1$ close to the cooling hole and $\eta = 0$ downstream. The effectiveness depends on a large number of parameters, most of theme associated with the flow topology of a jet into a cross flow. A jet issuing from a wall into a main stream is bent in the direction of the flow and develop into a pair of counter rotating vortices that pump low temperature fluid away from the wall and high temperature fluid close to the wall. Most of the research in cooling configurations are associated with ways to reduce the development of these counter rotating vortices such as trenches, shaped holes, compound angle holes and secondary anti-vortex holes.

The literature on gas turbine film cooling is vast and would take much more room to discuss than available for the

present article. The bibliographic listing up to 1996 alone takes 10 pages (Kercher, 1998). Only the studies relevant to this investigation will be presented in this introduction due to space limitations.

Initially the research on turbine blade film cooling addressed issues such as mass flow ratio, density ratio, temperature ratio, etc. In search of higher gain in cooling effectiveness, nowadays the investigations on film cooling are addressing the details of flow topology which recognizes the importance of the counter-rotating vortices resulting from the interaction of the cooling jets and the main stream. Detailed measurements taken by Bernsdorf *et al.* (2006) show the development of the vortical structures associated with the cooling jet. Latter the results presented by **?** are used to calibrate a computational model based on the RANS equations (burdet *et al.*, 2007).

Based on the investigations on the detailed flow topology new propositions are presented in the literature aiming at reducing the development of streamwise counter-rotating vortices. These investigations consider shaped holes and compound angle holes. An alternative for that end is to use anti-vortex holes (Heidmann and Ekkad, 2008) which are easier to manufacture. Recent experimental results regarding the anti-vortex hole positioning and orientation have been presented by Dhungel *et al.* (2009). They concluded that the anti-vortex hole position has a significant impact on the cooling performance.

A Detail numerical analysis was recently performed by Renze *et al.* (2009) addressing the issue of cooling jet topology in rows of holes using large eddy simulation (LSE). The results show that the mixing a the downstream rows have a different nature. The velocity gradients are lower downstream of the first row and the turbulence production is reduced. As a result the cooling effectiveness is significantly improved. The superior performance of LES in capturing the flow physics is reinforced and show strong variations in the turbulent Prandtl number.

Recently El-Gabry *et al.* (2010) discussed the penetration characteristics of film cooling jets at high blowing ratio using numerical methods. They compared the results with experimental data and discussed the shortcomings of numerical simulations for film cooling analysis. As other numerical simulations the cooling effectiveness is unpredicted due to the complexity of the problem of a jet into a cross flow stream. The main difficulty is the jet wake region, which is not well captured by the Reynolds average Navier-Stokes formulation with eddy vorticity closing.

Sakai *et al.* (2009) studied the reliability of detached eddy simulation (DES) and RANS turbulence models for the prediction of film cooling effectiveness. They compared four different turbulent models and showed adequate agreement for the laterally averaged film cooling effectiveness. The RANS model unpredicted the effectiveness lateral spreading.

The present investigation build on previous research on film cooling effectiveness in a system composed of rows of holes (Renze *et al.*, 2009; Dhungel *et al.*, 2009). Rows of holes are used to improve cooling in localized regions, but the interaction between rows may have an adverse effect on the cooling flow downstream. In order to investigate the interaction between different rows a system with two holes is studied where a smaller upstream hole is place in front of a larger hole. The interaction between the main stream and the upstream hole leads to the development of counter rotating vortices upstream of the second hole resulting in a different flow field downstream. The effect of blowing ratio and mass flow split between rows on the cooling effectiveness and cooling mass flow will be evaluated numerically.

A open source control volume solver (Open∇Foam) is used to solve the compressible Reynolds Average Navier-Stokes equations on a model configuration. Preliminary conclusions on film cooling effectiveness are presented and for the initial investigated configuration a negative effect on the cooling effectiveness is observed.

2. METHODOLOGY

The research presented in this paper was performed using Open∇Foam, an open source C++ library for computational fluid dynamics. The compressible Navier-Stokes equations are solved numerically based on a finite volume scheme. The turbulent stress terms were closed using a two equation turbulence model based on the Boussinesq turbulent viscosity hypothesis.

2.1 Mean flow equations

The compressible Navier-Stokes equations are decomposed using the Favre decomposition.

$$\phi \equiv \widetilde{\phi} + \phi'', \qquad \widetilde{\phi} \equiv \frac{\overline{\rho\phi}}{\overline{\rho}}, \qquad \text{such that} \quad \overline{\rho\phi''} = 0; \quad \overline{\rho\widetilde{\phi}} = \overline{\rho}\widetilde{\phi} = \overline{\rho\phi} \tag{1}$$

where the overbar (e.g. $\overline{\rho\phi}$) represents the Reynolds decomposition temporal average and ρ is the density.

The Favre decomposition is introduced in the governing equations and a temporal average is taken. For the pressure, internal energy and density the Reynolds decomposition is applied. The resulting equations are

$$\frac{\partial\overline{\rho}}{\partial t} + \frac{\partial}{\partial x_j}\left[\overline{\rho}\widetilde{u_j}\right] = 0, \tag{2}$$

$$\frac{\partial}{\partial t}(\overline{\rho}\widetilde{u_i}) + \frac{\partial}{\partial x_j}\left[\overline{\rho}\widetilde{u_i}\widetilde{u_j} + \overline{p}\delta_{ij} - \widetilde{\tau_{ij}}^{tot}\right] = 0, \tag{3}$$

$$\frac{\partial}{\partial t}(\overline{\rho}\widetilde{e_0}) + \frac{\partial}{\partial x_j}\left[\overline{\rho}\widetilde{u_j}\widetilde{e_0} + \widetilde{u_j}\overline{p} + \widetilde{q_j}^{tot} - \widetilde{u_i}\widetilde{\tau_{ij}}^{tot}\right] = 0. \tag{4}$$

where t is the time, u the velocity, x the spatial coordinate, p is the pressure and δ_{ij} the Kronecker delta.

The turbulent and laminar stresses are

$$\widetilde{\tau_{ij}}^{tot} = \widetilde{\tau_{ij}}^{lam} + \widetilde{\tau_{ij}}^{turb}, \qquad \widetilde{\tau_{ij}}^{lam} = \mu\left(\frac{\partial\widetilde{u_i}}{\partial x_j} + \frac{\partial\widetilde{u_j}}{\partial x_i} - \frac{2}{3}\frac{\partial\widetilde{u_k}}{\partial x_k}\delta_{ij}\right), \tag{5}$$

$$\widetilde{\tau_{ij}}^{turb} = -\widetilde{\overline{\rho u_i'' u_j''}} = \mu_t\left(\frac{\partial\widetilde{u_i}}{\partial x_j} + \frac{\partial\widetilde{u_j}}{\partial x_i} - \frac{2}{3}\frac{\partial\widetilde{u_k}}{\partial x_k}\delta_{ij}\right) - \frac{2}{3}\overline{\rho}k\delta_{ij}. \tag{6}$$

$k = 1/2\widetilde{u_i'' u_i''}$ is the turbulent kinetic energy, and μ_t is the turbulent viscosity, which will be evaluated with a turbulence model.

The laminar and turbulent heat fluxes are

$$\widetilde{q_j}^{lam} = -C_p\frac{\mu}{\mathrm{Pr}}\frac{\partial\widetilde{T}}{\partial x_j} = -\frac{\gamma}{1-\gamma}\frac{\mu}{\mathrm{Pr}}\frac{\partial}{\partial x_j}\left(\frac{\overline{p}}{\overline{\rho}}\right), \tag{7}$$

$$\widetilde{q_j}^{turb} = C_p\widetilde{\overline{\rho u_j'' T}} = -C_p\frac{\mu_t}{\mathrm{Pr}_t}\frac{\partial\widetilde{T}}{\partial x_j} = -\frac{\gamma}{1-\gamma}\frac{\mu_t}{\mathrm{Pr}_t}\frac{\partial}{\partial x_j}\left(\frac{\overline{p}}{\overline{\rho}}\right), \tag{8}$$

The average perfect gas relation results

$$\overline{p} = (\gamma-1)\,\overline{\rho}\left(\widetilde{e_0} - \frac{1}{2}\widetilde{u_k}\widetilde{u_k} - k\right). \tag{9}$$

where μ is the dynamic viscosity λ is the thermal conductivity, T is the static temperature, C_p is the specific heat at constant pressure and $\mathrm{Pr} = C_p\mu/\lambda$ is the laminar Prandtl number, R is the gas constant, γ is the specific heat ratio, C_v is the specific heat at constant volume, and e is the internal energy. The total energy is $e_0 = e + 1/2u_k u_k$. γ, C_p, C_v e R are assumed constant.

2.2 Turbulence modeling

For the Reynolds stress term the Boussinesq hypothesis is applied. The SST $k-\omega$ turbulence model is used (Menter, 1994). This model uses the $k-\omega$ formulation in the inner boundary layer, which integrates up to the viscous sub-layer region, and switches to a $k-\epsilon$ turbulence model away from the wall. The model is know to give reasonable results in adverse pressure gradient and separating flows. This model gives somewhat large values of turbulence close to stagnation regions, but this effect is less pronounced than with a $k-\epsilon$ model. The $k-\omega$ model implemented on Open∇Foam have been used for turbomachinery heat transfer problems and showed good performance (Mangani *et al.*, 2007).

$$-\rho\overline{u_i' u_j'} = 2\mu_t\overline{S_{ij}} - \frac{2}{3}\delta_{ij}\left(\mu_t\frac{\partial\overline{u_k}}{\partial x_k} + \rho k\right), \qquad \overline{S_{ij}} = \frac{1}{2}\left(\frac{\partial\overline{u_i}}{\partial x_j} + \frac{\partial\overline{u_j}}{\partial x_i}\right). \tag{10}$$

where k is the turbulent kinetic energy, $k = \overline{u_i' u_i'}/2$ and

$$\nu_t = \frac{a_1 k}{\max\left(a_1\omega, SF_2\right)} \tag{11}$$

F_2 and a_1 are closure coefficients.

The transport equations for k and ω as well as other details of the model can be found in Menter (1994).

2.3 Numerical method

The governing equations are solved numerically based on a cell centered unstructured finite volume scheme implemented on an open source code (Open∇Foam). The computational domain is composed of a rectangular domain with a flat plate at the lower surface where the cooling holes are placed as shown in Fig. 1.

The upstream hole is a square hole $D \times D$ where $D = 0.0127$ m and the downstream hole has twice the area of the upstream hole with sides $\sqrt{2}D$. The holes are distant $2D$ apart and the upstream hole is $5D$ from the leading edge. Downstream of the second hole there are $25D$ to the exit boundary.

The solution methodology is base on a segregated, compressible version, pressure based SIMPLE algorithm and a steady state solver. For pressure and velocity an algebraic multigrid solver with preconditioning is used and for the turbulent quantities and the energy equation a preconditioned, bi-conjugate gradient solver is used. The vector field is interpolated using a combination of Gauss-Gamma and Gauss linear schemes or a combination of Gauss linear scheme and first order Gauss upwind scheme.

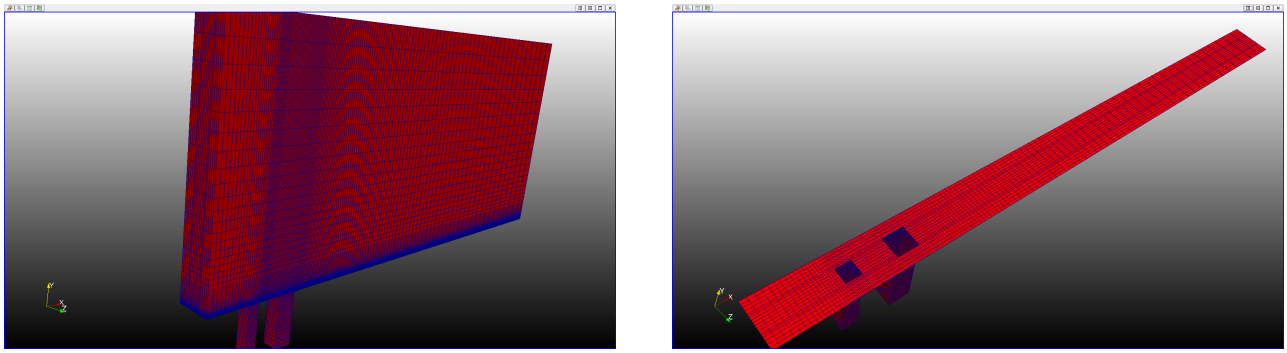

Figure 1. Topology and grid distribution

2.4 Boundary conditions

The following boundary conditions are imposed: at the top pressure and temperature are specified, $p = p_{\text{atm}} = 101325$ Pa and $T = T_\infty = 1000$ K. The velocity boundary condition is imposed as a inlet/outlet condition depending on the flow structure. At the inlet $p = p_{\text{atm}}$ and $T = T_\infty$. At the outlet zero gradient of all variables is imposed. At solid boundaries on the plate or on the cooling holes no slip condition is imposed for the velocity components, zero gradient for pressure and adiabatic wall for the energy equation. At the cooling holes inlet uniform temperature $T = 300$ K and mass flow are imposed. In the spanwise direction periodic boundary conditions are enforced. The initial field is given by the free-stream conditions for all variables. The mass flow on the cooling ducts are specified such that the main stream to cooling jet velocity ratio is 0.5, for a freestream velocity of 11 m/s.

Initial and boundary values for the turbulence quantities are crucial for the correct simulation of turbulent flows. They are a source of uncertainties and are usually unknown from experimental conditions.

Given the turbulent intensity I, a turbulent length scale L and the ratio μ_t/μ, the kinetic energy and the dissipation rate ϵ may be calculated:

$$k = \frac{3}{2}(\overline{u}I)^2, \quad \text{where} \quad I \equiv \frac{u'}{\overline{u}}, \quad \epsilon = C_\mu \frac{k^{\frac{3}{2}}}{L}, = C_\mu \frac{\rho k^2}{\mu} \left(\frac{\mu_t}{\mu}\right)^{-1}. \tag{12}$$

where C_μ is a fitting constant and the length scale is given as a percentage of the problem characteristic length. The turbulent intensity used for the present problem is equal to 1%. The characteristic length scale is $L = 0.07D$.

3. RESULTS

3.1 Validation test case

The appropriateness of Open∇Foam for gas turbine heat transfer analysis has been demonstrated by Mangani *et al.* (2007), who suggests the used of turbulence models which integrate the turbulent quantities down to the wall viscous sublayer. In order to check the assembling, grid resolution and solver choices for the present study comparisons were made with experimental and numerical results presented by Mahjoob and Rahni (2006). The topology and flow conditions presented by Mahjoob and Rahni (2006) are similar to the conditions used in the present investigation but a single cooling hole was used. Figures 2 and 3 present velocity distributions measured along the center line of the plate at different streamwise positions.

The results obtained with the configuration and grids used in the present study show good agreement with experimental and numerical results presented by Mahjoob and Rahni (2006). The discrepancies are due to the fact that in Mahjoob and Rahni (2006) paper there is no indication of the entry length from the leading edge to the position of the cooling hole. In the present runs the entry length is $5D$. Nevertheless the results are in good agreement.

3.2 Cooling results

The interference between two cooling jets change the cooling characteristics on the wall surface downstream. In the following sections the effect of an upstream hole on the wall cooling is investigated. The control parameter is the relation between the mass flow in the upstream hole and the downstream hole. Four configurations are studied, the first for a single cooling hole, the second for 30% of the total mass flow of the first configuration coming out of the upstream hole, the third for 10% and the last for 5%. The single hole case serves as a reference condition.

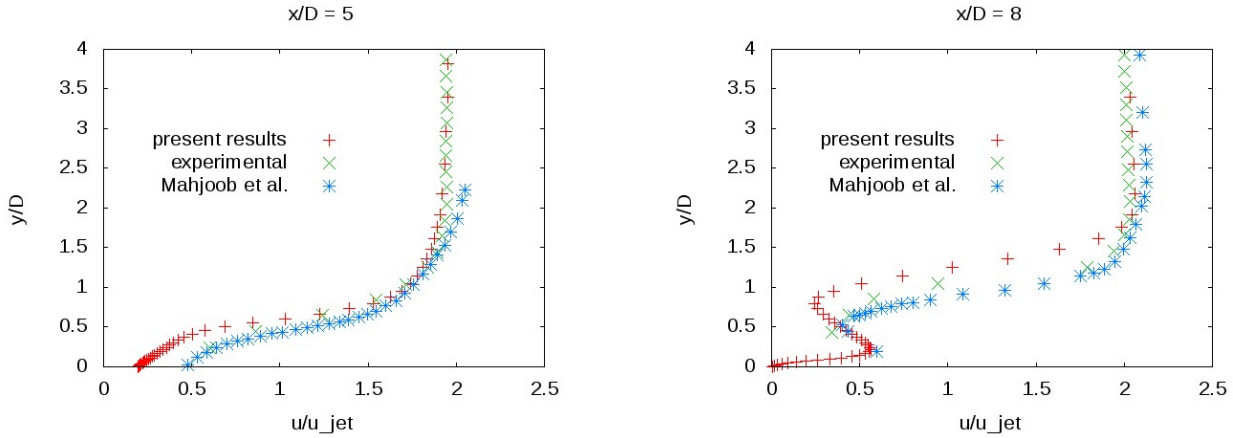

Figure 2. Validation Results. Comparisons with Mahjoob and Rahni (2006). Streamwise position $x/D = 5$ and 8.

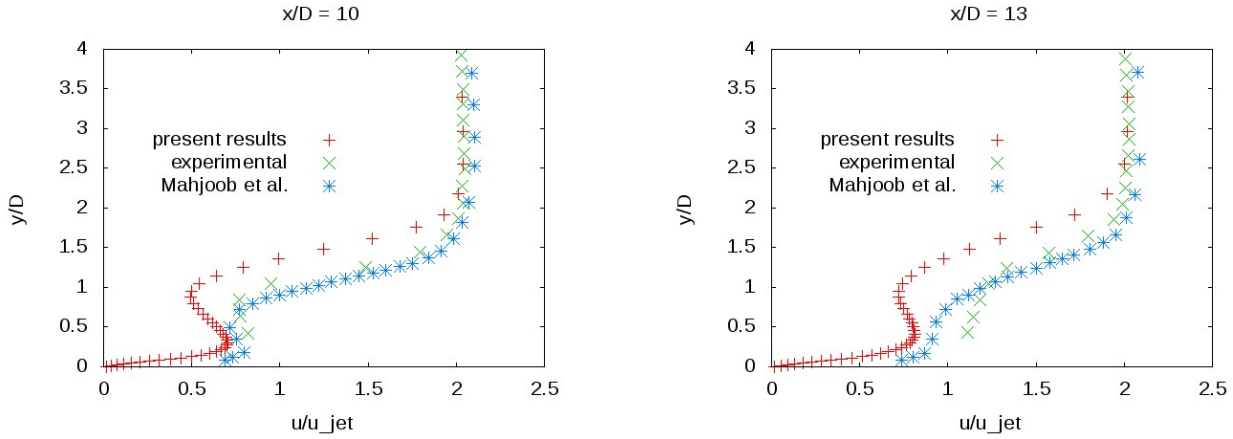

Figure 3. Validation Results. Comparisons with Mahjoob and Rahni (2006). Streamwise position $x/D = 10$ and 13.

3.2.1 Flow in a single hole

For a jet coming out of a cooling hole normal to the main stream direction the jet is bent in the direction of the main flow and the interaction between the two stream results in the development of counter-rotating vortices with a upwash region located in the center line of the plate. The flow structure is shown in the two first slides in figures 4 where plate temperature and streamlines are presented. The following two slides show a spanwise plane located $2D$ downstream of the second hole and the top view temperature distribution over the plate. The counter rotating vortices are clear on the streamlines and on the spanwise plane. The two higher temperatures on the side of the plate are due to this vortical system. On the either side of the plate the vortices form a downwash region, bringing hot fluid closer to the wall.

3.2.2 30% flow in the upstream hole

When 30% of the cooling flow comes out of the upstream hole one observes that the counter rotating vortices generated by it uplift the jet coming out of the downstream hole (Fig. 5). The resulting effect is that higher temperatures are observe over the entire plate and a stronger heating results in the region about $2D$ of the downstream hole and closer to the sides of the plate. The downwash effect of the downstream vortices is reinforced by the upstream vortices. The downstream jet is located exactly inside the upwash region of the first jet. This flow topology is significant when one considers rows of cooling holes located close to each other. Nether the near hole region is better cooled, nor the downstream region for the configuration tested. The streamlines resulting from both jets move away from the wall as a result of the upwash at the center line.

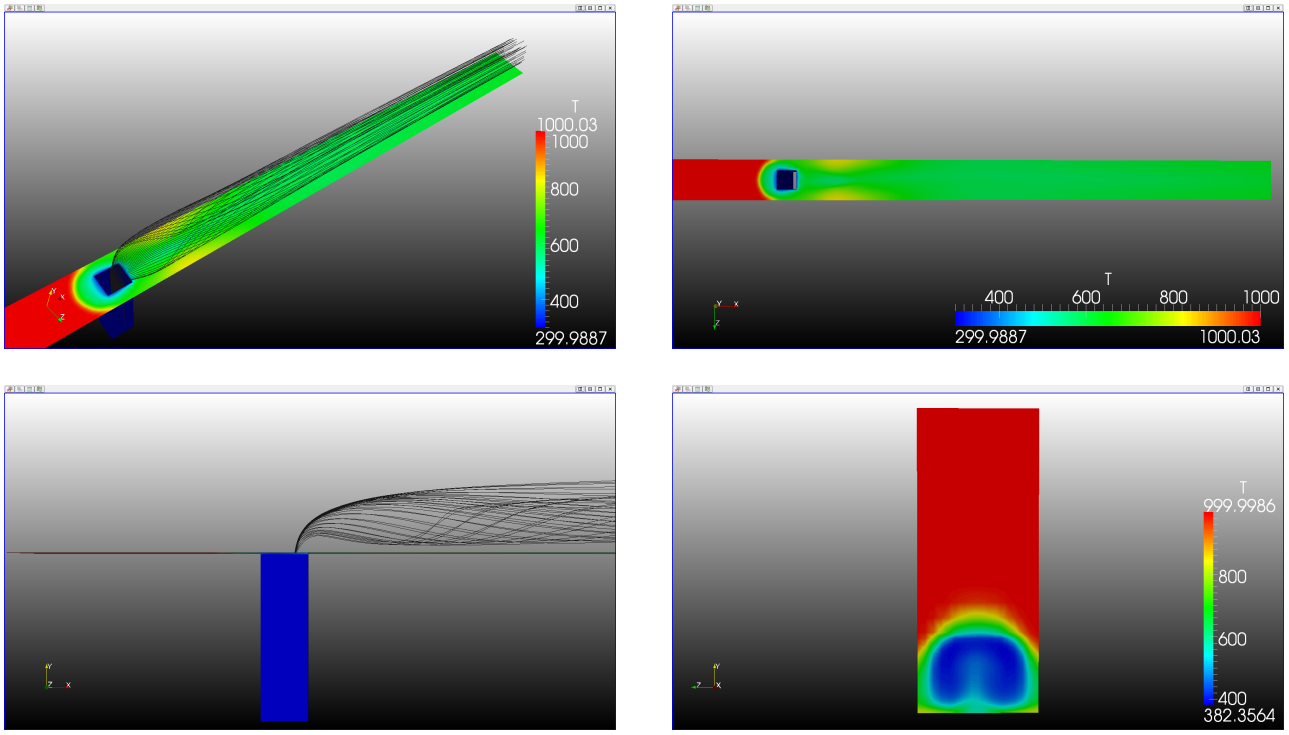

Figure 4. Flow in a single hole

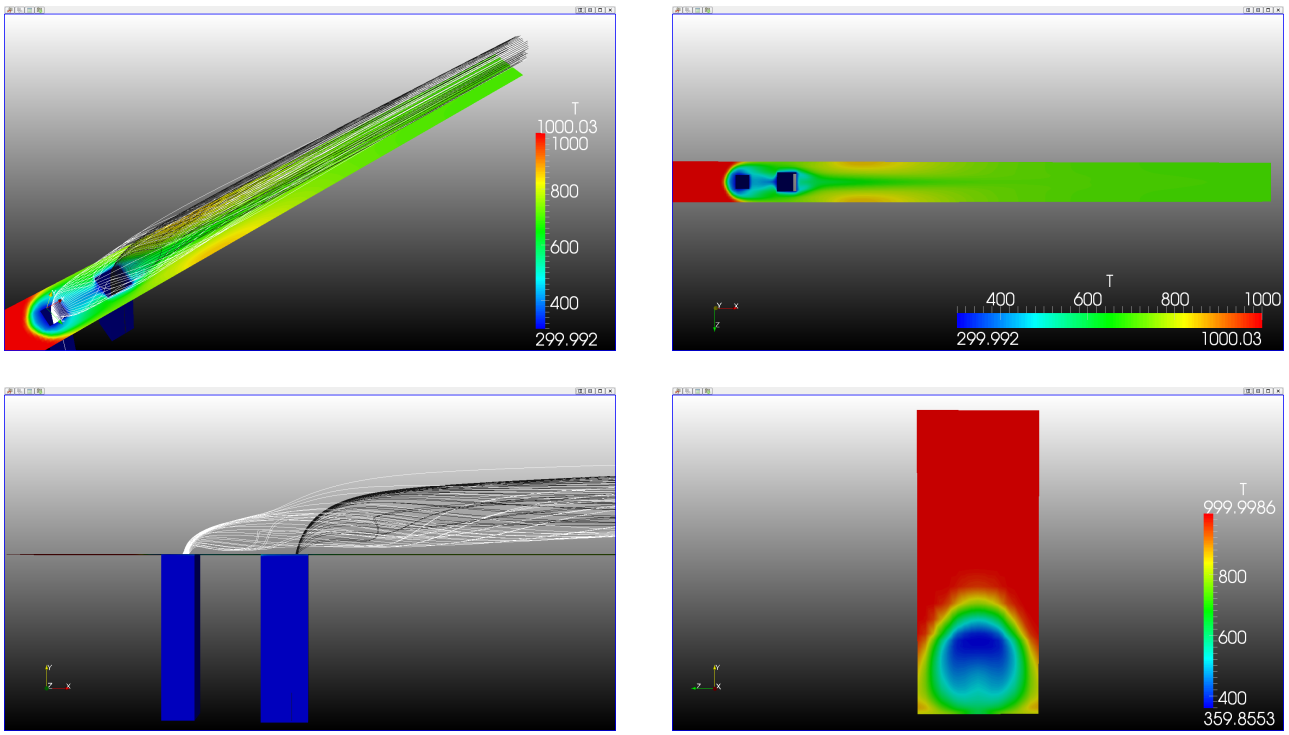

Figure 5. 30% mass flow in the upstream hole.

3.2.3 10% flow in the upstream hole

The initial idea for the present investigation was to have the upstream hole serve as a barrier for the downstream hole. The upstream jet would deflect the main flow from the downstream jet. The intended result would be to reduce the counter rotating vorticity of the downstream hole and enhance the plate cooling. In order to test this idea the third test case considers a weaker upstream jet in order to avoid the effect observed in the previous case where the upstream hole uplifted the main downstream cooling jet. The results presented in Fig. 6 show that a weaker jet upstream mixes with the downstream jet without lifting it up. A better cooling is observed in the plate between the two jets and significant cooling is also observed downstream. Nevertheless the waist line temperature about $2D$ from the downstream jet is higher than that observed for the single jet. Temperature distribution in the center line will be compared in the following sections to access the differences in cooling capacity.

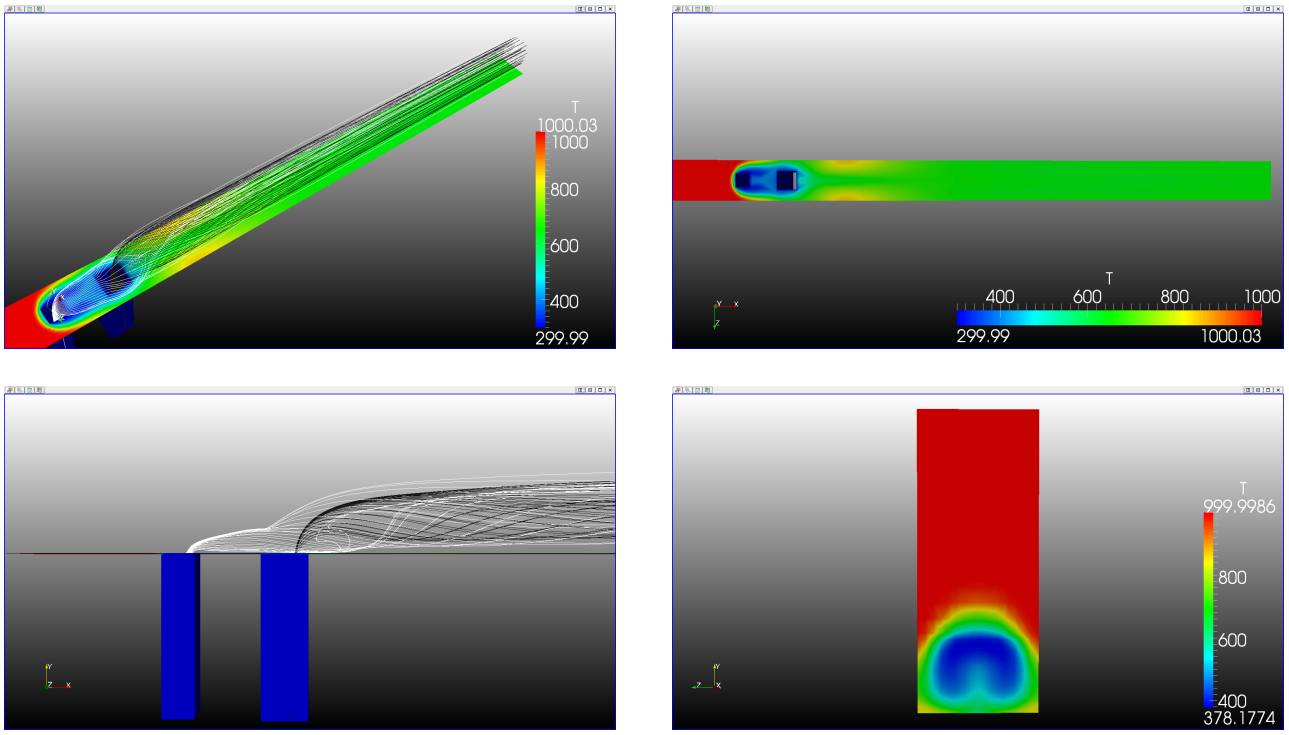

Figure 6. 10% mass flow in the upstream hole.

3.2.4 5% flow in the upstream hole

Reducing further the mass flow in the upstream hole one can observe that the first jet stays close to the wall and interfere with the downstream jet only in that region. The cooling ability for this configuration is compared with the previous one in the following section but the cross stream plane show that the counter rotating vorticity does not change much from that of the single hole. The streamlines from the upstream hole go around the downstream jet and cooler fluid from the upstream hole is trapped under the downstream vortices as a result of the downwash flow on the sides of the plate.

3.3 Temperature distribution

In order to quantify the cooling characteristics for the different cooling configurations the temperature distribution along the center line of the plate and along the side boundary are plotted (Fig. 8. The results show that downstream of the second hole the lower plate temperature correspond to the case with a single hole. The upstream hole has a detrimental effect in all configurations test. Nonetheless, when the mass flow in the upstream flow is of the order of 10% of the total mass flow or less, the resulting temperature does not change significantly from the temperature given by the single hole configuration. The benefit of the upstream hole is associated with the increased cooling in the region between holes when the mass flow in the upstream hole is less than 10% of the total cooling flow. When cooling configurations composed of rows of holes are considered the present results should be taken into account when trying to optimize the cooling effect on the plate.

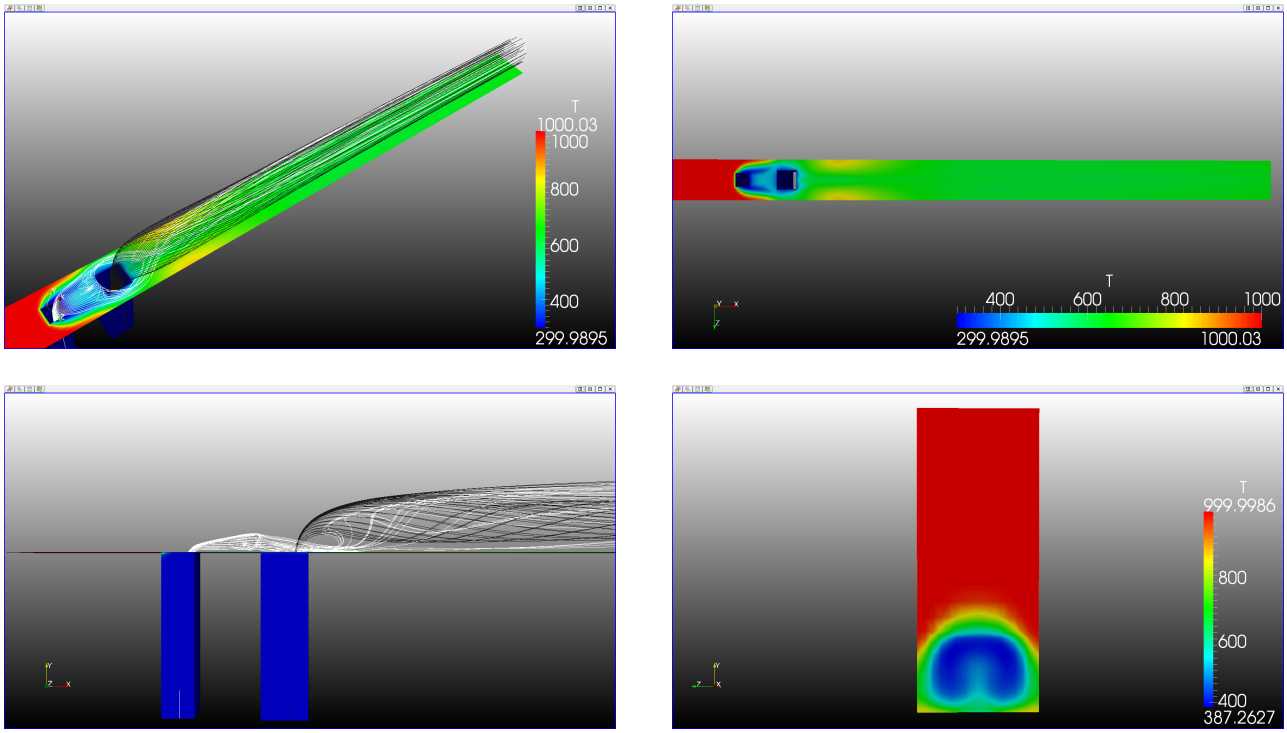

Figure 7. 5% mass flow in the upstream hole.

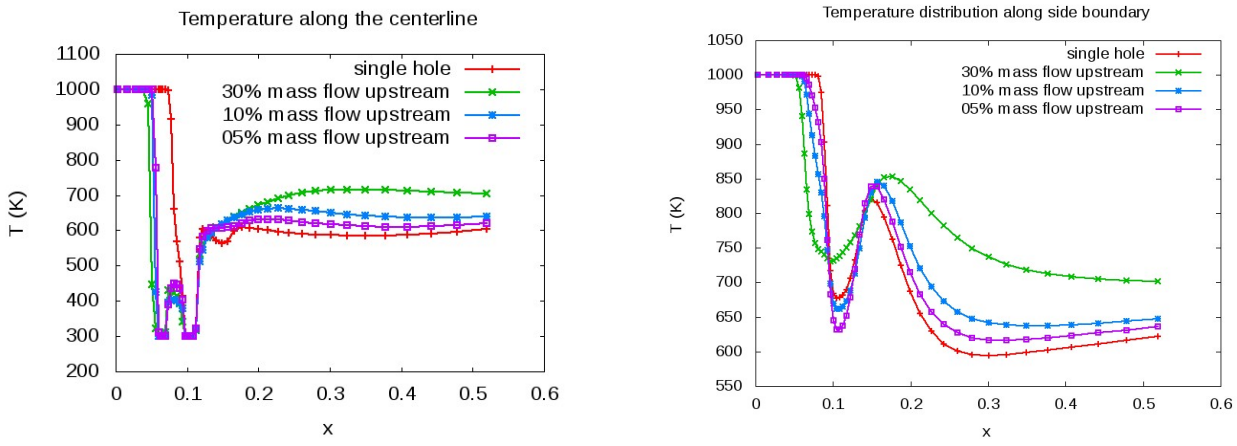

Figure 8. Temperature distribution along de center line and along de side boundary.

3.4 Flow separation

The streamlines presented on the previous sections show flow separation close to the jets. In order to compare the strength of this flow separation for the different configurations the following figures show the velocity magnitude on a (x, y) plane along the center line. Flow separation is observed for all configurations upstream of the main cooling hole and the least severe separation is that of the single hole configuration. The presence of the upstream hole results in a stronger region of separated flow downstream of the main cooling jet. The separation region is due to the blockage effect of the jet.

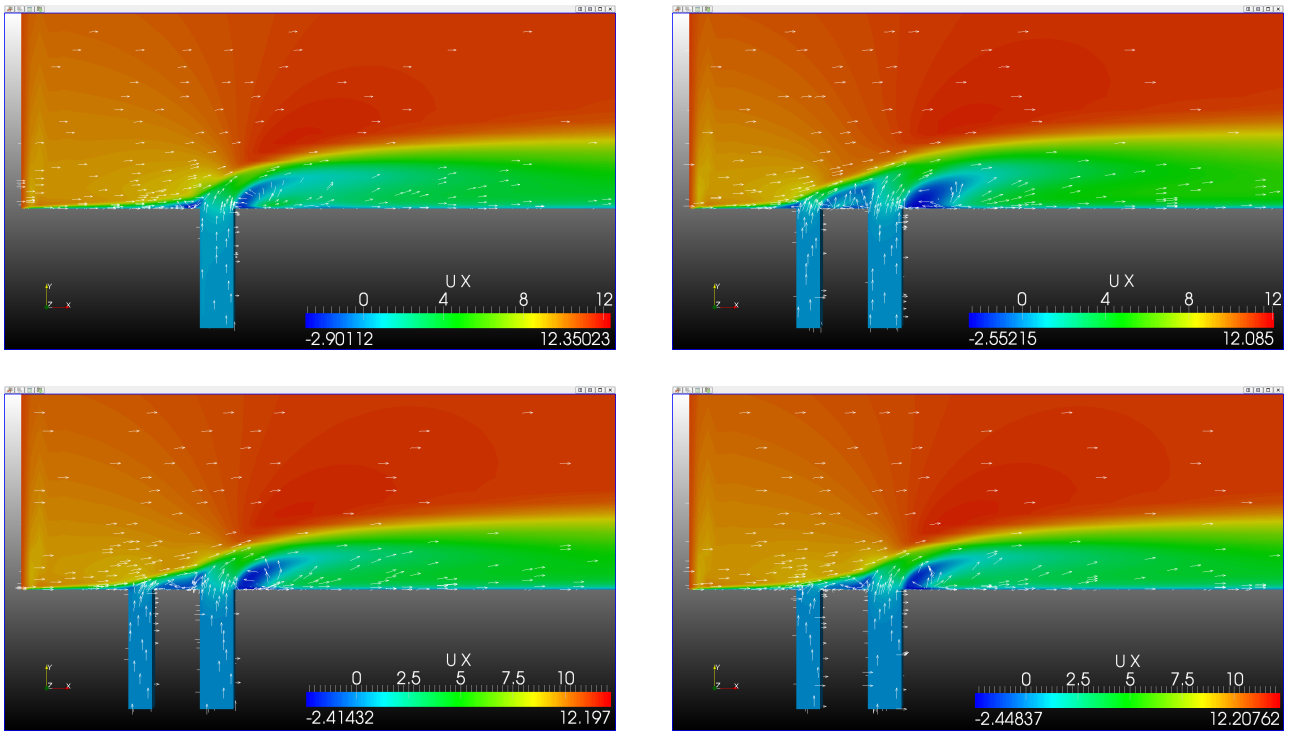

Figure 9. Velocity magnitude in the center line plane.

4. CONCLUSION

In the present investigation a system of two cooling holes was investigated numerically using an open source software package for CFD analysis (Open∇Foam). The interaction between the two cooling jets is such that placing an upstream hole upstream of the main cooling hole has a detrimental effect on downstream cooling. The upstream hole vorticity uplift the downstream jet away from the wall resulting in higher wall temperatures. For small mass flow on the upstream hole this effect is not strong due to the dominance of the downstream jet vorticity which traps the upstream jet close to the wall. Another benefit of the small mass flow upstream hole is the better cooling in the region between holes.

5. ACKNOWLEDGMENTS

The authors would like acknowledge the support from VSE – Vale Soluções em Energia.

6. REFERENCES

Bernsdorf, S., Rose, M. and Abhari, R.S., 2006. "Modeling of film-cooling—part i: Experimental study of flow structure". *Journal of Turbomachinery*, Vol. 128, pp. 141–149.

burdet, A., Abhari, R.S. and Rose, M.G., 2007. "Modeling of film-cooling—part ii: Model for use in three-dimensional computational fluid dynamics". *Journal of Turbomachinery*, Vol. 129, pp. 221–231.

Dhungel, A., Lu, Y., Phillips, W., Ekkad, S.V. and Heidmann, J., 2009. "Film cooling from a row of holes supplemented with antivortex holes". *Journal of Turbomachinery*, Vol. 131, pp. 021007–1–021007–10.

El-Gabry, L., Heidmann, J. and Ameri, A., 2010. "Penetration characteristics of film cooling jets at high blowing ratio". *AIAA Journal*, Vol. 48, No. 5, pp. 1020–1024.

Heidmann, J. and Ekkad, S.V., 2008. "A novel antivortex turbine film cooling hole concept". *Journal of Turbomachinery*, Vol. 130, No. 3, pp. 686–698.

Kercher, D., 1998. "A film-cooling cfd bibliography: 1971–1996". *International Journal of Rotating Machinery*, Vol. 4, No. 1, pp. 61–72.

Mahjoob, S. and Rahni, M.T., 2006. "Parameters affecting turbulent film cooling–reynolds average navier stokes computational simulation". *Journal of Thermophysics and Heat Transfer*, Vol. 20, No. 1, pp. 92–100.

Mangani, L., Bianchini, C., Andreini, A. and facchini, B., 2007. "Development and validation of a c++ object oriented cfd code heat transfer analysis". In *Proceedings of the ASME Thermal Engineering and Summer Heat Transfer Conference*. Vancouver, Canada, Vol. AJ-1266.

Menter, F.R., 1994. "Two equation eddy-viscosity turbulence models for engineering applications". *AIAA Journal*, Vol. 32, No. 8, pp. 1598–1605.

Renze, P., Schroder, W. and Meinke, M., 2009. "large-eddy simulation of interacting film cooling jets". In *Proceedings of the ASME Turbo Expo 2009*. Orlando, Florida, USA, Vol. GT2009-59164.

Sakai, E., Takahashi, T., Funazaki, K., Salleh, H.B. and Watanabe, K., 2009. "large-eddy simulation of interacting film cooling jets". In *Proceedings of the ASME Turbo Expo 2009*. Orlando, Florida, USA, Vol. GT2009-59517.

7. Responsibility Notice

The authors are the only responsible for the printed material included in this paper